GENOME EDITING

Efficient modification of *CCR5* in primary human hematopoietic cells using a megaTAL nuclease and AAV donor template

Blythe D. Sather,[1]* Guillermo S. Romano Ibarra,[1]* Karen Sommer,[1] Gabrielle Curinga,[1] Malika Hale,[1] Iram F. Khan,[1] Swati Singh,[1] Yumei Song,[1] Kamila Gwiazda,[1] Jaya Sahni,[1] Jordan Jarjour,[2] Alexander Astrakhan,[2] Thor A. Wagner,[3,4] Andrew M. Scharenberg,[1,4,5†] David J. Rawlings[1,4,5†]

Genetic mutations or engineered nucleases that disrupt the HIV co-receptor CCR5 block HIV infection of CD4$^+$ T cells. These findings have motivated the engineering of *CCR5*-specific nucleases for application as HIV therapies. The efficacy of this approach relies on efficient biallelic disruption of *CCR5*, and the ability to efficiently target sequences that confer HIV resistance to the *CCR5* locus has the potential to further improve clinical outcomes. We used RNA-based nuclease expression paired with adeno-associated virus (AAV)–mediated delivery of a *CCR5*-targeting donor template to achieve highly efficient targeted recombination in primary human T cells. This method consistently achieved 8 to 60% rates of homology-directed recombination into the *CCR5* locus in T cells, with over 80% of cells modified with an MND-GFP expression cassette exhibiting biallelic modification. MND-GFP–modified T cells maintained a diverse repertoire and engrafted in immune-deficient mice as efficiently as unmodified cells. Using this method, we integrated sequences coding chimeric antigen receptors (CARs) into the *CCR5* locus, and the resulting targeted CAR T cells exhibited antitumor or anti-HIV activity. Alternatively, we introduced the C46 HIV fusion inhibitor, generating T cell populations with high rates of biallelic *CCR5* disruption paired with potential protection from HIV with CXCR4 co-receptor tropism. Finally, this protocol was applied to adult human mobilized CD34$^+$ cells, resulting in 15 to 20% homologous gene targeting. Our results demonstrate that high-efficiency targeted integration is feasible in primary human hematopoietic cells and highlight the potential of gene editing to engineer T cell products with myriad functional properties.

INTRODUCTION

HIV entry into human T cells requires binding to both CD4 and one of several G protein (heterotrimeric guanine nucleotide–binding protein)–coupled chemokine receptors that act as co-receptors for HIV infection. CCR5 is the major co-receptor used by transmitted HIV-1 viruses (*1*). Highlighting the importance of CCR5 in HIV infection, a naturally occurring human *CCR5* allele conferring HIV resistance creates a protein variant (CCR5 Δ32) that is nonfunctional (*2*–*4*). One strategy for treating HIV-infected patients is the use of engineered nucleases to disrupt CCR5 expression in patient T cells. Patients reinfused with autologous T cells after *CCR5* disruption with zinc-finger nucleases (ZFNs) showed improved CD4 T cell survival during HIV viremia induced by temporary cessation of antiretroviral drugs (*5*). The key to the method's success is that CCR5 expression appears to be dispensable for normal immune responses, as evidenced in individuals who are homozygous for the *CCR5* Δ32 allele. Thus, biallelic disruption of *CCR5*, desirable for effective HIV resistance, should not adversely affect T cell function. This feature also makes the *CCR5* locus a potentially advantageous site to target for other genetic T cell therapies because this site does not affect cell survival or growth and is within open, transcriptionally active chromatin. Coding sequences that might be usefully targeted to this locus would include, but not be limited to, agents previously shown to help control or eradicate HIV (*6*).

Gene editing relies on the use of engineered nucleases to induce double-strand breaks (DSBs) in specific target genes. DSBs are repaired by endogenous cellular enzymes through one of two pathways: nonhomologous end joining (NHEJ), an error-prone pathway that results in a high frequency of nucleotide insertions or deletions (indels), or homology-directed repair (HDR), which seamlessly repairs DSBs by using homologous DNA as a template. HDR can be subverted to insert nonhomologous DNA into specific DSB sites by using an exogenous donor template, with the desired nonhomologous sequence flanked with homologous ones. Although for some applications, the goal of gene editing is to disrupt gene function by creating indel mutations, in other cases, HDR is required to insert a novel coding sequence or to repair a gene mutation.

Therapeutic application of HDR requires both an engineered, site-specific nuclease and an efficient method for transient delivery of this nuclease and a relevant DNA donor template into primary cells. We have described a hybrid nuclease platform that combines a transcription activator–like effector (TALE) DNA binding domain with an engineered, sequence-specific homing endonuclease (HE), referred to as a megaTAL (*7*). These nucleases promote efficient cleavage of

[1]Center for Immunity and Immunotherapies and Program for Cell and Gene Therapy, Seattle Children's Research Institute, Seattle, WA 98101, USA. [2]Bluebird Bio, Seattle, WA 98102, USA. [3]Center for Global Infectious Disease Research, Seattle Children's Research Institute, Seattle, WA 98101, USA. [4]Department of Pediatrics, University of Washington, Seattle, WA 98101, USA. [5]Department of Immunology, University of Washington, Seattle, WA 98101, USA.
*These authors contributed equally.
†Corresponding author. E-mail: andrewms@u.washington.edu (A.M.S.); drawling@uw.edu (D.J.R.)

genomic DNA (gDNA) with high sequence specificity, and the single megaTAL coding sequence can be efficiently delivered by mRNA transfection, allowing high-level transient expression. When HDR is the desired outcome, a suitable donor DNA template that satisfies key criteria must also be optimized. These criteria are that it must be easy to deliver and nontoxic to primary cells; it should be efficiently recognized as a candidate repair template by the HDR machinery; and it should not integrate randomly into the host chromatin. Here, we describe the optimization of gene editing at the *CCR5* locus of primary human T cells, using a *CCR5*-specific megaTAL and recombinant adeno-associated virus (rAAV) delivered donor template. The resulting protocol allowed us to efficiently target a range of expression constructs to the *CCR5* locus in primary T cells and adult mobilized $CD34^+$ peripheral blood stem cells (PBSCs).

RESULTS

Activity of alternative nucleases editing the human *CCR5* locus

Site-specific insertion of therapeutic coding sequences in primary cells via HDR requires efficient delivery of both a high-efficiency designer nuclease and a DNA donor template. In addition, we hypothesized that overhang architecture at the nuclease cleavage site might differentially bias DSB repair toward either HDR or NHEJ. We tested this idea for two alternative nuclease platforms that efficiently target the *CCR5* locus: a megaTAL nuclease (CCR5 megaTAL; fig. S1) that generates 3′ DNA overhangs or a CCR5–TALEN (TALE nuclease) pair where a dimerized Fok1 nuclease creates 5′ overhangs. We used reagents that targeted the same region of *CCR5* (Fig. 1A) to optimally compare rates of HDR.

To verify that both nucleases efficiently targeted the *CCR5* locus, we used polyadenylate-tailed mRNA to deliver nuclease or a blue fluorescent protein (BFP) mRNA (as transfection control) into prestimulated purified primary human $CD4^+$ T cells. Samples receiving BFP control RNA were 98% transfected as measured by FACS 48 hours after transfection. In the absence of a repair template, DNA breaks are resolved by the error-prone NHEJ pathway, resulting in either seamless religation or indels. We first estimated indel frequency at the *CCR5* locus using the T7 endonuclease assay [Fig. 1B; (*8*)] and detected about two times greater activity with CCR5-TALEN as with megaTAL (82% versus 44%, respectively). Because the T7 assay may underestimate NHEJ events in the presence of a uniform spectrum of indels, we also assessed NHEJ rates using tracking of indels by decomposition (TIDE) sequencing [Fig. 1B and fig. S2; (*9*)]. TIDE sequencing allows the quantitation and characterization of mutations within a capillary sequence analysis relative to a reference sequence analysis by using a decomposition algorithm. Using this assay, we observed a rate of 42 and 32% NHEJ (TALEN versus megaTAL, respectively). Thus, NHEJ rates in primary T cells were equivalent or slightly higher with the CCR5-TALEN versus megaTAL.

To first test whether these nucleases facilitate HDR repair, we used the TLR assay (*10*). In this assay, the CCR5-megaTAL and CCR5-TALEN binding and cleavage sites were inserted within the GFP coding sequence of the GFP-T2A-mCherry expression cassette, and lentiviral delivery was used to stably introduce this TLR cassette into the chromatin of HEK 293T cells (HEK-CCR5-TLR). Reporter lines were treated with gene-editing reagents (including various doses of an AAV.GFP repair template) followed by flow cytometry at 72 hours to simultaneously detect NHEJ (read as indels causing frame shift mutations that allow mCherry expression) and HDR (read as repaired GFP expression; downstream mCherry is out of frame; Fig. 1C). Transfection of HEK-CCR5-TLR cells with BFP mRNA alone, or with the AAV.GFP donor alone, did not affect GFP or mCherry expression (Fig. 1D). HEK 293T cells transfected with TALEN mRNA alone exhibited 3.9 times higher NHEJ rates than did cells treated with megaTAL alone. Although NHEJ rates dropped ~50% for both enzymes when AAV.GFP donor template was present, the NHEJ rates of the TALEN remained about threefold higher than those of the megaTAL at all AAV doses. Notably, although the CCR5-TALENs exhibited higher NHEJ rates, HDR events were similar at all AAV dosages in megaTAL- and TALEN-treated cells [or slightly higher for the megaTAL at 50,000 multiplicity of infection (MOI)]. On the basis of these data, we calculated a more than threefold higher HDR/NHEJ ratio (at all AAV MOIs, with the exception of the highest) when cutting was performed by the megaTAL than by the TALEN enzyme.

High-efficiency HDR at the *CCR5* locus in primary T cells

Having established the efficiency of our nucleases, we next tested methods for transient delivery of a DNA donor template into primary human T cells using recombinant AAV. To identify an optimal AAV serotype, we transduced enriched primary human CD4 T cells using self-complementary (sc) AAV.MND.GFP [scAAV expressing GFP downstream of the modified retroviral promoter/enhancer (MND)] packaged using seven different AAV serotypes: 1, 2, 2.5, 5, 6, 8, and DJ. AAV transduction was read out as transient GFP expression at 48 hours (fig. S3), and maximal expression was achieved with virus packaged with serotype 6 at all AAV doses.

To assess HDR at the *CCR5* locus in primary human T cells, we generated AAV6-serotyped vectors containing an MND-GFP expression cassette inserted between 1.3 kb (kilobase) *CCR5* homology arms (adjacent to the region containing both the megaTAL and TALEN cleavage sites; AAV.CCR5.GFP; Fig. 2A). A control AAV containing an MND-BFP expression cassette without homology arms (AAV.BFP) was also generated to track rates of non–homology-driven AAV insertion at gDNA breaks. We tested multiple parameters for combining CCR5-megaTAL mRNA transfection with AAV transduction to optimize both cell viability and HDR (stable GFP expression over time) including the following: timing and sequence of cell stimulation, transfection and transduction, and incubation temperature after transfection. We found robust HDR using the sequence of procedures shown in Fig. 2A (see also Materials and Methods); we refer to the nuclease mRNA transfection (preceding the AAV donor template transduction) as time 0 of gene editing. Using optimized conditions, the percentage of cells transfected with BFP mRNA was 98% at day 2 and decreased to <1% by day 16. Expression of the fluorochrome, in AAV.BFP- or AAV.CCR5.GFP-only–transduced cells, averaged 80 and 64%, respectively, after 2 days (Fig. 2, B and C). This expression was unstable over time (presumably because of the presence of episomal AAV), decreasing to <1 and 2% for AAV.BFP or AAV.CCR5, respectively, by day 16. In contrast, in cells treated with both megaTAL mRNA and AAV.CCR5.GFP donor, high-level GFP expression was present at early time points (81% at day 2) and decreased somewhat over time. Consistent with stable integration of the donor template into host chromatin, most cells maintained robust GFP expression (63% at day 16). To determine whether stable GFP expression resulted from HDR or from direct insertion of the AAV DNA into the *CCR5* cleavage site, we tested whether *CCR5* homology arms were required. Cells were transduced with an AAV.BFP construct lacking homology arms. Although a large fraction of cells were positive for BFP at day 2 (86%), this

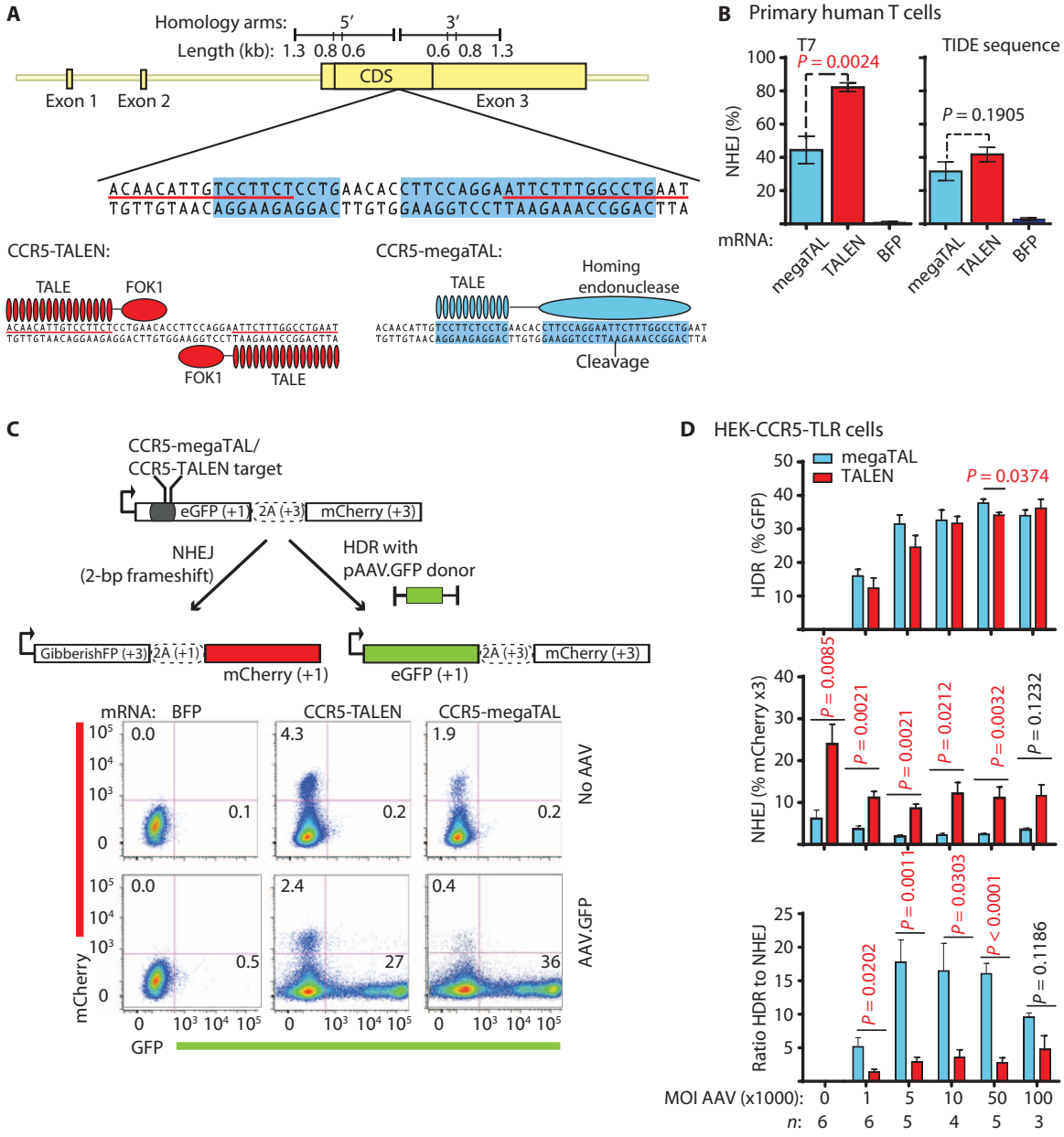

Fig. 1. CCR5-TALEN and CCR5-megaTAL activity in T cells and comparison of NHEJ and HDR events in a TLR reporter line. (**A**) Location of the CCR5-TALEN (red line) and CCR5-megaTAL nuclease (blue highlight) binding sites within the human *CCR5* gene. Nuclease architecture at the target site is schematically diagrammed beneath. *CCR5* sequence used as homology arms in donor templates in subsequent figures is indicated at top. (**B**) Percentage of NHEJ events in primary human T cells detected using the T7 and TIDE sequencing 18 to 21 days after transfection with megaTAL, TALEN, or BFP control mRNA (1 μg of each mRNA and 1 μg of RNA per TALEN monomer) ($n = 5$). (**C**) Schematic diagram of traffic light reporter (TLR) cassette and representative data showing fluorescent marker expression based on repair pathway. Translational reading frame is indicated in parenthesis for each coding sequence. Fluorescence-activated cell sorting (FACS) plots beneath show green fluorescent protein (GFP) and mCherry expression in representative CCR5 TLR assay. GibberishFP, open reading frame (ORF) encoded by out-of-frame translation of GFP; eGFP, enhanced GFP. (**D**) HDR versus NHEJ events at *CCR5* TLR locus in human embryonic kidney (HEK) 293T cells after treatment with CCR5-megaTAL or CCR5-TALEN mRNA and increasing MOI of AAV.GFP repair template. Bars show the means ± SEM; significance was calculated using the unpaired two-tailed *t* test; *P* values <0.05 are in red. CDS, coding sequences; FOK1, *Flavobacterium okeanokoites* nuclease.

proportion decreased to ~7% by day 16. Although more BFP$^+$ cells at day 16 were observed in the presence of the megaTAL (7% versus <1%), indicative of on-target insertion events, together these data indicated that most of the cells with sustained GFP expression after megaTAL and AAV.CCR5.GFP co-delivery likely underwent HDR (Fig. 2C).

To confirm the occurrence of HDR, we amplified gDNA from untreated cells or from cells treated with megaTAL mRNA (with or without

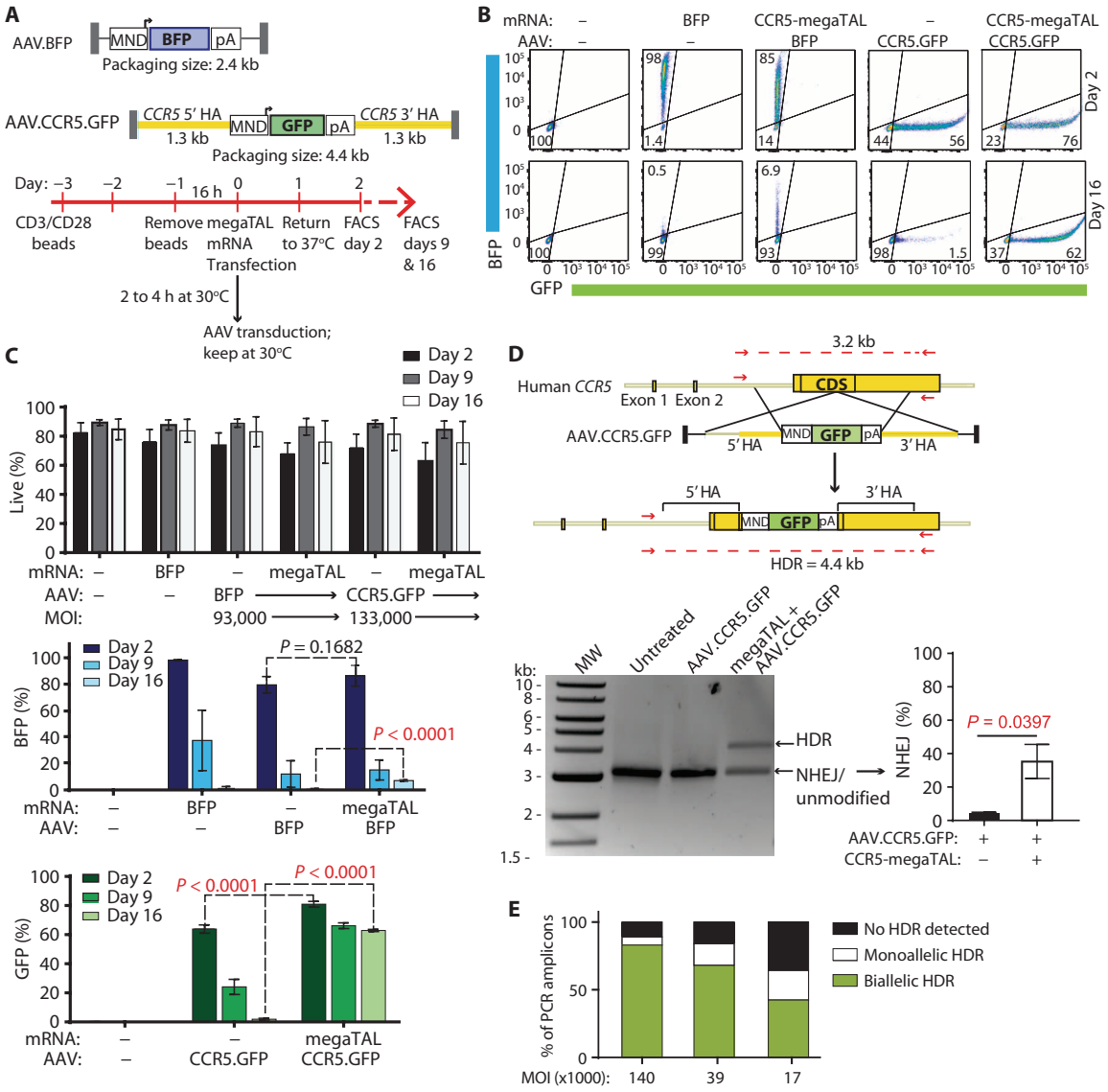

Fig. 2. Efficient HDR in primary T cells leading to introduction of a GFP expression cassette within the *CCR5* locus. (**A**) (Top) Diagram of AAV constructs used as donor templates. (Bottom) Timeline of gene-editing procedure beginning with bead stimulation of $CD4^+$ T cells. pA, SV40 polyadenylation signal; HA, homology arm. (**B**) Representative flow cytometry plots showing BFP versus GFP expression at days 2 and 16 after gene editing. The percentage of live single lymphocytes within the relevant quadrant is indicated. (**C**) Cell viability and BFP and GFP expression over time after gene editing ($n = 5$). Significance was calculated using the unpaired *t* test with the Holm-Sidak correction for multiple comparisons; significant *P* values (<0.05) are in red. (**D**) Diagram of human *CCR5* locus before and after HDR with the AAV.CCR5.GFP donor template. Primers binding outside homology arms were used to amplify gDNA from treated cells visualized on agarose gel; expected sizes of bands for unedited and edited alleles are indicated; right chart shows indel % (determined by TIDE sequencing) within the lower–molecular weight (MW) bands ($n = 3$). *P* value was calculated using the unpaired two-tailed *t* test. (**E**) Nested polymerase chain reaction (PCR) of single cells (31 to 100 cells per condition) edited using megaTAL and AAV.CCR5.GFP donor at indicted MOIs. Graph shows percentages of amplicons with a single higher–molecular weight band (biallelic HDR) and a single lower–molecular weight band (no HDR detected) or both bands (monoallelic HDR).

the AAV.CCR5.GFP donor template) using oligonucleotides targeted to sequence outside of the *CCR5* homology arms (Fig. 2D). Whereas gDNA from all cells produced bands that matched the size of the wild-type allele (or alleles with small indels), we also detected a band that matched the size predicted for HDR-modified loci in cells treated with both the donor template and CCR5-megaTAL. The products of PCRs were cloned into plasmids and colonies sequenced to confirm the presence of HDR-modified alleles (fig. S4). Colony sequencing of PCR products also confirmed the presence of viral insertions within the *CCR5* locus when AAV.BFP was used in place of AAV.CCR5.GFP as a donor template after megaTAL treatment (fig. S4). This amplification strategy was also used in single-cell PCR studies to estimate the frequency of biallelic and monoallelic HDR achieved with our gene-editing protocol. We identified amplicons consistent with biallelic HDR events

in 42% of GFP$^+$-engineered T cells at the lowest MOI of the AAV donor, and the frequency of biallelic events increased to 82% at our maximum MOI (Fig. 2E). Although CD4 T cells are the primary targets for therapeutic disruption of *CCR5*, the ability to target genes to the *CCR5* locus has applications in both CD4 and CD8 T cells. For example, CD4-specific applications include introduction of gene products that limit HIV entry, processing, or integration; applications in CD8 cells include targeted introduction of chimeric antigen receptors (CARs). We thus tested the efficacy of this *CCR5* gene–editing protocol in total CD3- and in CD8-enriched human peripheral blood cells. We observed similar high rates of HDR and similar viability in CD3-, CD4-, or CD8-enriched T cells that underwent our *CCR5*-editing protocol (fig. S5).

Integration-deficient lentivirus (IDLV) delivery has previously been used to facilitate HDR in hematopoietic cells (*11*, *12*). We therefore also tested HDR rates using IDLV designed to deliver a GFP donor template. Initial studies in the HEK-CCR5-TLR reporter cell line showed that IDLV delivery of the GPF repair template resulted in lower HDR rates in comparison with AAV delivery (fig. S6A). Consistent with this finding, IDLV containing the CCR5.GFP reporter cassette also led to only a low level (0.5%) of stable GFP expression in primary T cells (fig. S6, B and C).

The coding sequence of *CCR5* shares high sequence identity (74%) to that of *CCR2*, particularly within the region encoding the seven transmembrane domains (84%), where the megaTAL and TALEN target sites are located. Sequences within *CCR2* and *KIAA1257* (an uncharacterized gene) were identified as potential megaTAL off-targets on the basis of homology to the *CCR5* target site combined with the CCR5-megaTAL one-off specificity profile (*13*). We thus tested whether *CCR5* gene editing resulted in off-target cleavage or HDR at the *CCR2* locus. Quantification of indels at the potential target site in *CCR2* by TIDE sequencing showed that NHEJ rates for the megaTAL and TALEN here were 21.8 and 1.8%, respectively, compared with 42% at the *CCR5* locus for both (fig. S7A). Indels were not detected at *KIAA1257* by TIDE analysis (fig. S7A). Similar to these findings, an early iteration of the ZFN now in clinical trials for *CCR5* disruption also exhibited off-target activity within *CCR2* (*14*). Despite off-target activity at *CCR2*, neither HDR nor capture of the AAV.CCR5.GFP donor events was detected at the *CCR2* locus by PCR analysis (fig. S7B).

Comparison of HDR rates using the CCR5-megaTAL or CCR5-TALENs

Using our optimized procedures, we compared the HDR efficacy with CCR5-megaTAL to that with TALENs in primary T cells. We transfected primary CD4 T cells with mRNA to express either the CCR5-megaTAL (1 μg of RNA) or both TALEN half-sites (1 μg of RNA for each half-site), followed by AAV.CCR5.GFP at a range of dosages or by an AAV.BFP control (Fig. 3, A and B). Cell viability throughout the experiment was not significantly different between cells treated with the megaTAL or TALEN (Fig. 3B). Expression of the AAV.BFP control was also equivalent in megaTAL- and TALEN-treated cells, indicating that AAV transduction, expression, and insertion rates were independent of the nuclease used (Fig. 3B). We found higher GFP expression at all dosages of AAV and at each time point analyzed with the CCR5-megaTAL. Direct comparison of the proportion of cells with sustained GFP expression (day 16) revealed a 1.3- to 4.5-fold increase (across all AAV doses) using megaTAL versus the TALEN mRNA (Fig. 3, C and D). Because the CCR5-megaTAL nuclease uses a single coding sequence (a potentially important cost consideration in clinical application) and generates higher rates of HDR with less donor template in these studies, we pursued further characterization of gene targeting to the *CCR5* locus using this platform.

Maintenance of TCR diversity and sustained engraftment of gene-edited T cells

To determine whether our gene-editing protocol targets T cells representing a broad T cell receptor (TCR) repertoire, we analyzed the TCR spectratype of cells that had undergone gene editing using the CCR5-megaTAL and AAV.CCR5.GFP repair template. Edited cells were collected 8 to 16 days after gene editing for this analysis. We found that treatment with either CCR5-megaTAL alone or CCR5-megaTAL with AAV.CCR5.GFP had no substantial impact on the total TCR complexity of the sample. The complexity scores for each Vβ subfamily were also unchanged (Fig. 4A and fig. S8).

We next tested the ability of gene-edited T cells to engraft immunedeficient, nonobese diabetic–severe combined immunodeficient–interleukin-2 receptor (IL-2R)γ^{null} (NSG) mice. T cells treated with the CCR5-megaTAL alone, or in combination with AAV.CCR5 GFP, were injected into NSG mice 8 days after gene editing. One month after injection, lymphocytes were collected from the spleen and bone marrow for analysis. Mice remained healthy throughout this period with no overt signs of graft-versus-host disease by coat appearance or weight loss. An average of 18% of splenocytes recovered from all treatment groups were CD4$^+$ CD45$^+$ human lymphocytes, with no statistically significant differences in percentage or absolute number between recipients of gene-edited versus those of mock-treated cells. The MOI of the AAV.CCR5.GFP donor used in these experiments was 59,000; therefore, the input cells transplanted were about 30% GFP$^+$. This proportion of GFP$^+$ cells was only slightly reduced after 1 month in vivo, indicating that edited cells maintained long-term viability (Fig. 4B). There was no correlation between % GFP-modified cells in vivo and the number of human CD45$^+$ splenocytes (Fig. 4C). HDR was confirmed with PCR and colony sequencing (Fig. 4D). There was a 39% reduction in CCR5$^+$ CD4$^+$ splenic lymphocytes in recipients of CCR5-megaTAL only when compared to mock-treated cells, suggesting that altered CCR5 expression did not affect in vivo viability. An even greater reduction in CCR5 expressing CD4$^+$ cells was observed in mice receiving cells treated with both megaTAL and AAV donor, with 52 and 70% reduction in CCR5 surface expression in GFP$^-$ and GFP$^+$ cells, respectively.

Ex vivo *CCR5* gene editing in adult mobilized CD34$^+$ cells

The ability to target genes to the *CCR5* locus in CD34$^+$ cells is an important goal for therapies aimed at hematopoietic diseases including HIV. We optimized the use of our *CCR5* gene–editing reagents for mobilized CD34$^+$ cells apheresed from adult human volunteers. As seen in T cells, AAV serotype 6 enabled the highest delivery of scAAV.GFP expression (fig. S3). Optimal HDR and cell viability were observed when the timing of mRNA transfection and AAV transduction was reversed compared to our T cell protocol, a result of the slower cell cycling of the CD34$^+$ cell population. Additionally, although it increased our transfection efficiency, incubating the cells at 30°C greatly reduced CD34$^+$ cell viability. Using conditions optimized for the CD34$^+$ cells (Fig. 5A), 89% of cells expressed the BFP mRNA control 1 day after transfection (Fig. 5B). However, cells receiving the CCR5-megaTAL mRNA had NHEJ rates of only ~16% by TIDE sequencing, suggesting that CCR5-megaTAL activity is reduced in CD34$^+$ cells in comparison to primary T cells and/or that

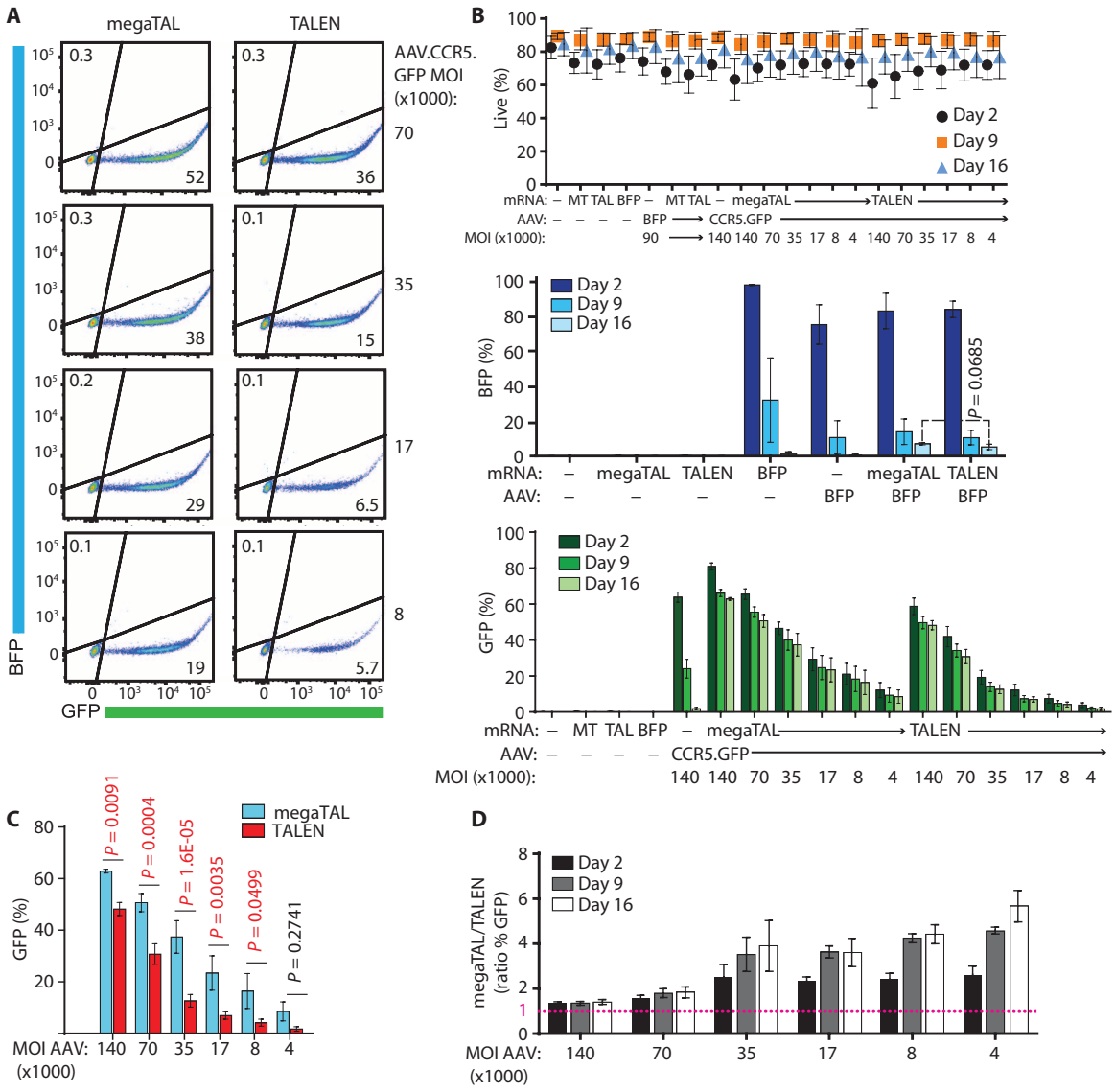

Fig. 3. Comparison of HDR rates in human primary T cells with CCR5-megaTAL versus those with CCR5-TALENs. (**A**) Representative FACS plots showing HDR events observed 16 days after treatment with CCR5-megaTAL versus those with CCR5-TALEN at varying MOI of the AAV.CCR5.GFP donor. The percentage of live single lymphocytes within a relevant quadrant is indicated. (**B**) Time course of cell viability (top), % BFP^+ cells (middle), and % GFP^+ cells (bottom) after treatment with control BFP (1 μg), CCR5-megaTAL (MT; 1 μg), or CCR5-TALEN (TAL; 1 μg of each TALEN half-site) mRNA with and without various MOI of the AAV.CCR5.GFP donor (or negative control AAV.BFP lacking *CCR5* homology arms). (**C**) Comparison of % GFP 16 days after gene editing with CCR5-megaTAL versus that with TALEN at various MOI of AAV.CCR5.GFP donor template. (**D**) Ratio of % GFP^+ cells after megaTAL- versus that of TALEN-mediated HDR over time and at various MOI of the AAV donor. All bars show means ± SEM of $n = 5$; significance was calculated using unpaired *t* test with the Holm-Sidak correction for multiple comparisons; *P* values (<0.05) are in red.

this population promoted more efficient DSB seamless repair. Transduction with AAV.CCR5.GFP alone resulted in 16% of cells expressing GFP at day 4, but GFP was undetectable by day 10. Co-delivery of megaTAL mRNA and CCR5 AAV donor resulted in 35% GFP expression at day 4 and 14% sustained GFP expression at day 10. Higher AAV.CCR5.GFP expression with nuclease co-delivery at day 4 likely results from disruption of cell cycling due to electroporation and/or nuclease-mediated DNA breaks, thus delaying dilution of episomal AAV. Notably, the viability of $CD34^+$ cells was more affected by the combination of AAV transduction and megaTAL transfection than that of T cells (Fig. 5, C and D). The presence of HDR events was verified by colony sequencing of PCR-amplified gDNA from cells receiving the gene-editing reagents (Fig. 5E).

Delivery of genetic therapies to the *CCR5* locus in primary human T cells

Clinical trials disrupting CCR5 expression in HIV patient autologous T cells are currently underway. We tested the capacity to simultaneously disrupt the *CCR5* locus and insert an expression cassette for candidate HIV therapeutics into the *CCR5* locus, an approach anticipated to

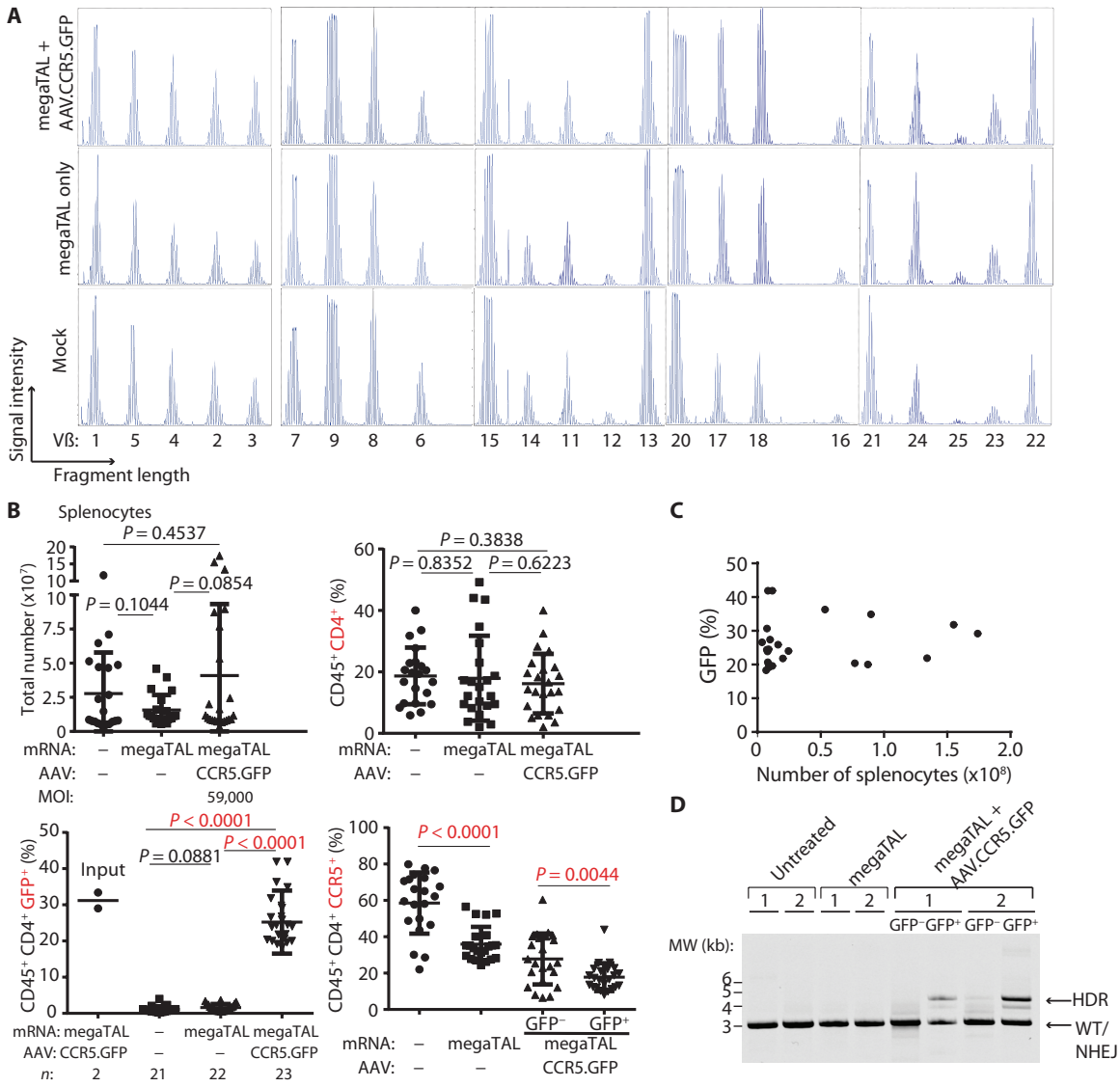

Fig. 4. Maintenance of TCR diversity and sustained engraftment of gene-edited T cells. (**A**) Representative TCR spectratypes of Vβ subfamilies 1 to 25 in mock-treated T cells (bottom panel) or T cells 8 to 19 days after treatment with CCR5-megaTAL mRNA with and without AAV.CCR5.GFP donor. (**B**) Total number and relative percentage of CD4 lymphocytes (upper panels), GFP$^+$ CD4 lymphocytes (lower left panel), and CD4$^+$ CCR5$^+$ lymphocytes (lower right panel) obtained from spleens of NSG mice 4 weeks after transfer of gene-edited T cells; numbers of mice for each condition is shown below *x* axis of GFP$^+$ panel and is the same for all panels. Bars show the means ± SEM; *P* values were calculated using the unpaired two-tailed *t* test; *P* values <0.05 are in red. *n* = number of mice. (**C**) % GFP variation versus splenocyte number for each mouse receiving CCR5-megaTAL and AAV.CCR5.GFP donor–edited T cells. (**D**) gDNA from total splenocytes obtained from two recipient mice for each condition at 4 weeks after T cell transfer was PCR-amplified using primers outside of the donor template homology arms and run on an agarose gel. The predicted size of HDR-modified (4.4 kb) and NHEJ/unmodified alleles (3.2 kb) are indicated. Splenocytes from mice receiving T cells edited with megaTAL and AAV.CCR5.GFP donor co-delivery were flow-sorted before obtaining gDNA to detect HDR and NHEJ events in GFP$^+$ and GFP$^-$ cells. WT, wild-type.

enhance the clinical use of *CCR5* disruption. Previous studies have shown that expression of the HIV restriction protein C46 protects cells from infection by HIV (*15*, *16*) and may offer protection against HIV strains with CXCR4 tropism. We designed a donor template to test whether we could engineer C46 expression into targeted CD3 T cells (Fig. 6A). Notably, our preliminary analysis introducing fluorescent reporters suggested that decreasing homology arm lengths to 0.6 kb decreased HDR rates by ~30% (fig. S9). The homology arms used in this vector were 0.8 kb, the maximum length we could include while remaining within the AAV packaging size limit. Sixteen days after gene editing, 28% of T cells expressed GFP linked by the T2A cleavage peptide; C46 expression at the cell surface was confirmed with the monoclonal antibody (mAb) 2F5. We next designed a second-generation anti–HIV-CAR gene repair construct on the basis of a high-affinity broadly neutralizing HIV antibody [PGT145; (*17*)]. The HIV-CAR included the single-chain variable fragment of PGT145 upstream of both CD3ζ peptide and CD137 (4-1-BB)

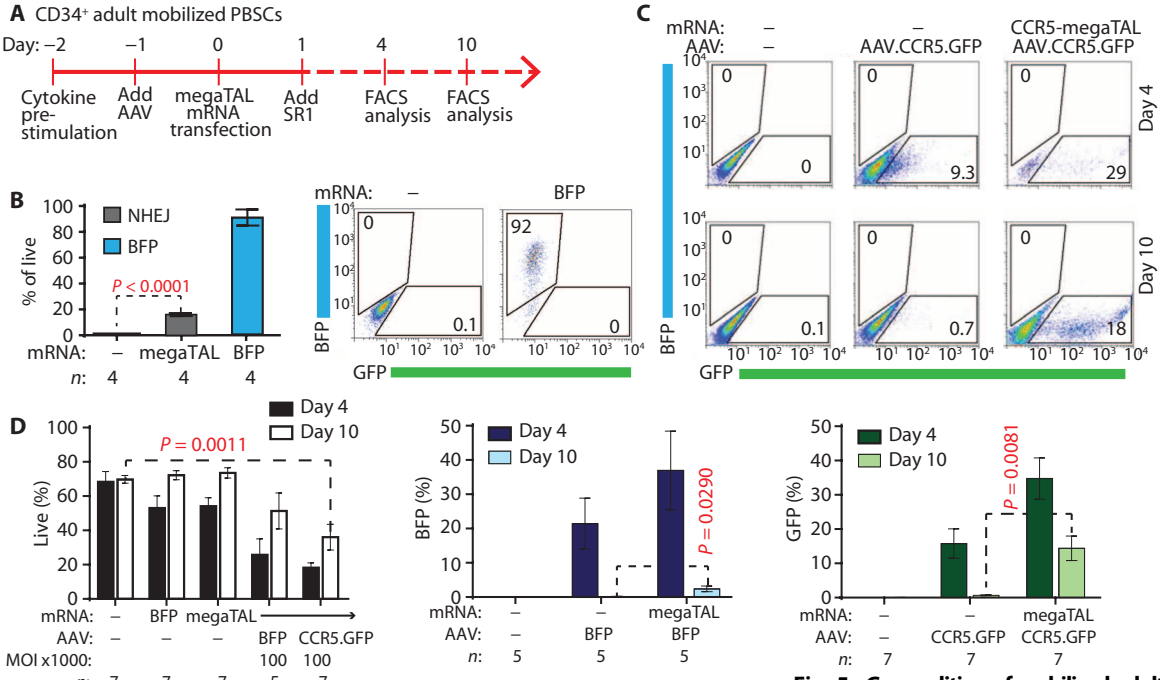

Fig. 5. Gene editing of mobilized adult CD34$^+$ cells using co-delivery of megaTAL and AAV.CCR5.GFP donor. (**A**) Timeline of CD34$^+$ cell gene-editing procedures and analyses. (**B**) (Left) % NHEJ events detected (by TIDE sequencing) 10 days after treatment with megaTAL mRNA and % of cells separately transfected with BFP mRNA 24 hours after transfection. (Right) representative flow plots (gated on live singlets) showing BFP expression 24 hours after transfection. (**C**) Representative flow analysis (gated on live singlets) of BFP and GFP expression in CD34$^+$ cells transduced with the AAV.CCR5.GFP template with and without CCR5-megaTAL mRNA transfection at 4 and 10 days post-transduction. (**D**) Viability and % BFP$^+$ and GFP$^+$ CD34$^+$ cells after treatment with the specified gene-editing reagents. (**E**) DNA gel of PCR-amplified gDNA obtained from gene-edited CD34$^+$ cells. Predicted sizes of HDR-modified (4.4 kb) and NHEJ/unmodified alleles (3.2 kb) are indicated. Chart shows the indel % (by TIDE sequencing) within the lower–molecular weight band (n = 3). All P values were calculated using the unpaired two-tailed t test; n = number of independent experiments, performed using cells from two donors.

costimulatory domains (Fig. 6B). Downstream of the HIV-CAR protein, we placed a T2A peptide linked to an RQR8, a peptide consisting of epitopes derived from both CD34 and CD20 (*18*). RQR8 allows for the enrichment of cells expressing the HIV-CAR with commercially available clinical-grade anti-CD34 affinity beads (whereas the CD20 antigen can be used as a suicide gene in the presence of rituximab). As a candidate therapeutic CAR in the clinical setting of B cell malignancies in subjects with HIV, as well as positive control for target cell killing assays, we also created a donor template to express an anti–CD19-CAR and T2A-BFP cassette (Fig. 6C). Targeted insertions of anti–HIV-CARs and anti–CD19-CARs at day 16 were 14 and 9% in CD3 T cells as assessed by anti-CD34 and BFP expression, respectively. Anti–HIV-CAR cells were enriched by sorting on anti-CD34 beads, leading to 40% stable RQR8 expression, and similarly, anti–CD19-CAR cells were sorted for BFP expression, achieving a stable 51% expressing population. We verified the functional ability of our engineered T cells to become activated and to lyse target cells downstream of CAR antigen binding. First, we incubated edited or mock control CD3 T cells with cell lines stably expressing either HIV envelope or CD19 (Fig. 6D), observing that engineered T cells up-regulated the activation marker CD137 only when incubated with cells expressing their target antigen. We then tested the ability of CD19-CAR$^+$ T cells to lyse K562 cells expressing either CD19 and cis-linked GFP or a nonspecific target [B cell maturation antigen (BCMA)] and near-infrared fluorescent protein (iRFP) (a 1:1 ratio of CD19 target cell to irrelevant target expressing cell; Fig. 6E). Although the ratio of GFP$^+$/iRFP$^+$ target cells was not significantly altered in the presence of anti–CD19-CAR$^-$ T cells, addition of anti–CD19-CAR$^+$ T cells resulted in complete loss of GFP$^+$ target cells at effector/target ratios of 3:1 or greater, confirming that *CCR5* gene–edited T cells maintain the ability to respond to CAR engagement and direct cell killing in vitro. PCR

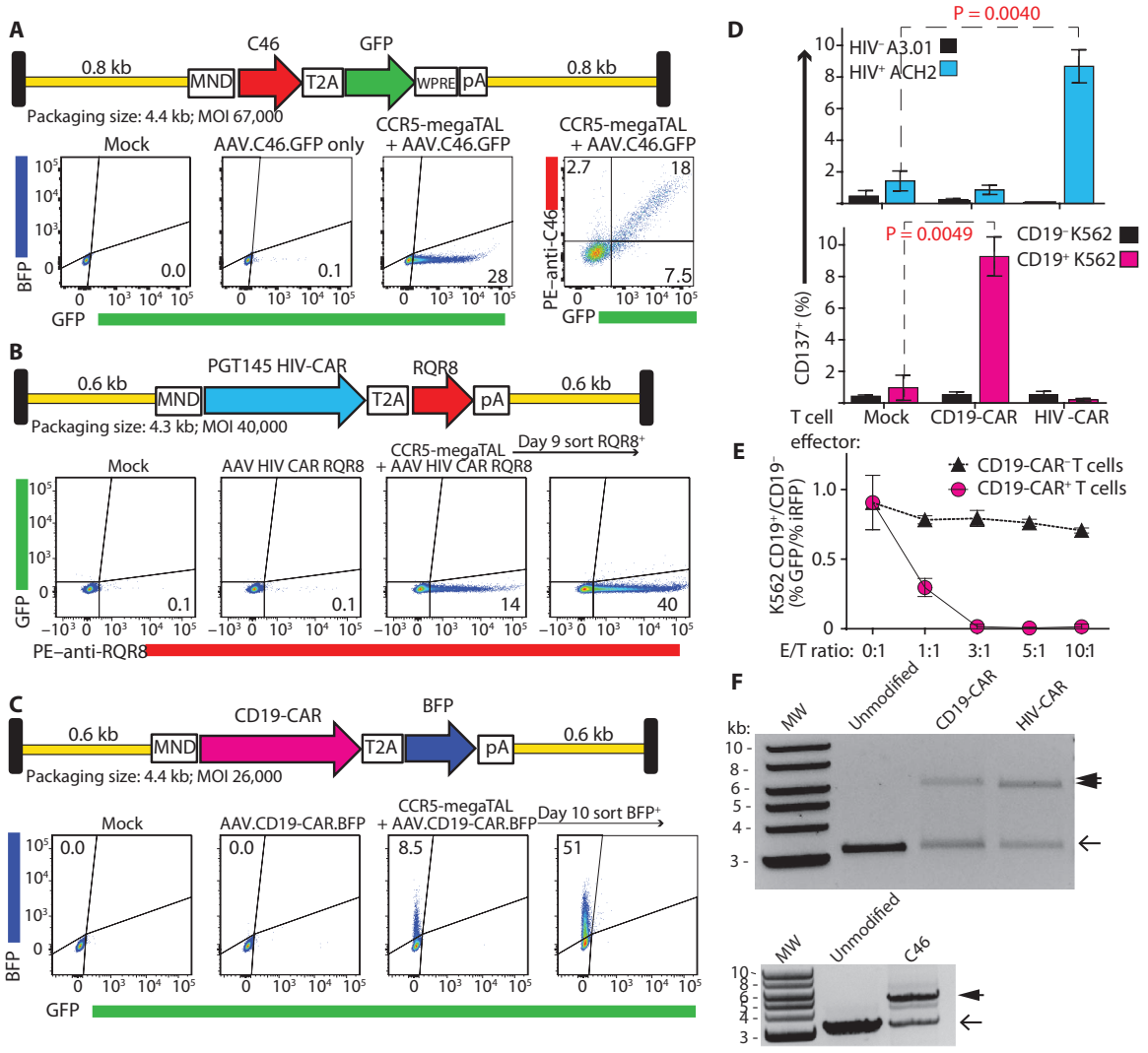

Fig. 6. Efficient expression of genetic therapies targeted to the *CCR5* locus in primary CD3 T cells. (**A** to **C**) AAV donor templates used to target C46 (A), HIV-CAR (B), and CD19-CAR (C) to the *CCR5* locus, including viral packaging size and MOI. FACS plots show expression 16 days after gene editing. For each, we show negative controls that were mock-transfected or transduced with only the AAV donor and the % of cells in relevant quadrant for transgene expression. HIV-CAR and CD19-CAR populations were column- or sort-purified before analysis at day 16. (**D**) CD137 expression in engineered T cells (*x* axis) cultured for 24 hours in the presence (blue or pink bars) or absence (black bars) of target cells expressing their indicated cognate antigen; *P* values were calculated using the unpaired two-tailed *t* test, and significant *P* values (<0.05) are in red; $n = 3$ independent experiments using T cells from different subjects. (**E**) Selective loss of GFP$^+$ CD19–expressing K562 target cells (T) relative to CD19$^-$ iRFP$^+$ K562 cells (*y* axis) 48 hours after treatment with CD19-CAR$^+$ T cell effectors (E) (ratio of E/T indicated on the *x* axis); $n = 3$. (**F**) DNA gels showing PCR amplicons of gDNA using primers binding outside of the *CCR5* homology arms. gDNA was obtained from T cells edited with the AAV donors diagrammed in (A), after purification by flow cytometry. Predicted sizes of HDR-modified alleles (CD19-CAR.T2A.BFP, 6.4 kb; HIV-CAR.T2A.RQR8, 6.3 kb; C46.T2A.GFP, 6.0 kb) are indicated by arrowheads at the right; open arrow indicates size of unmodified allele (3.2 kb). WPRE, woodchuck hepatitis virus posttranscriptional regulatory element; PE, phycoerythrin.

amplification of the *CCR5* allele verified the presence of bands consistent with HDR using the C46 and CAR donor templates (Fig. 6F).

DISCUSSION

Effective clinical application of gene editing requires efficient and safe methods for modification of primary human cell populations including hematopoietic cell lineages. The capacity to achieve HDR in primary cell populations, however, has lagged behind the recent rapid advancements in nuclease engineering. Here, we describe a cell engineering platform capable of driving high levels of gene editing in primary human T cells and CD34$^+$ hematopoietic stem cell (HSC) through the use of transient co-delivery of nuclease mRNA and a single-stranded rAAV donor template. Identification of an optimal DNA donor platform for use in primary hematopoietic cells, in parallel with careful timing and optimization

of mRNA delivery, allowed us to successfully apply editing technologies. We show that rAAV serotype 6 comprises an excellent DNA donor system that exhibits relatively limited toxicity in T cells, as measured by cell viability, even in the setting of very high MOI. Using this co-delivery method, we found both high cell viability and high levels of HDR in primary T cells with both megaTAL and TALENs. Most important, our methods easily introduced clinically relevant gene products into the *CCR5* locus in T cells, pointing to a potentially safe clinically translatable gene-editing platform.

The HDR rates described in this study in primary T cells are very high. To date, using 14 independent donors in 25 separate experiments, we observed an average knock-in rate of the MND-GFP cassette of 60% (range, 52 to 71%; SD, 4.9%). Single-cell molecular analysis of megaTAL-modified cells demonstrated high levels of biallelic HDR in cells expressing the GFP cassette, with rates greater than 80% at our highest level of AAV delivery. Similar HDR rates were observed in bulk CD3 as well as in enriched CD4 or CD8 T cell populations. Further, there was little loss of cell viability during co-delivery or subsequent culture manipulation. The engineered cells retained a broad TCR repertoire, consistent with modification of multiple independent cells, and exhibited sustained genomic modification without loss or altered competitive advantage in vivo in the NSG model. In comparison to our findings, a previous study assessed HDR in primary T cells using DNA transfection of ZFNs and donor, finding ~5% modification of *IL2Rγ* [reported as 20% on the basis of a correction for transfection efficiency; (*19*)]. Other work in human T cells has focused primarily on gene disruption. Plasmid delivery using Cas9 and guide RNAs led to NHEJ rates of <5% using a single guide and up to ~35% with multiple-guide delivery (*20*). Notably, the authors reported that primary cells, in contrast to transformed lines, were highly sensitive to plasmid-based DNA delivery, consistent with activation of innate DNA sensing pathways. mRNA-based nuclease delivery, as described here, also avoids the potential for insertion of a nuclease coding cassette into the cell genome, a scenario that could lead to genomic instability through accumulation of off-target cleavage events. mRNA has previously been used to deliver TALENs for TCR disruption, followed by lentiviral delivery of a CAR (*21*). TCR knockout frequency (~50%), however, was lower than the *CCR5* disruption rates achieved here with TALEN and megaTAL reagents, and as discussed below, our co-delivery method allowed both the desired CCR5 knockdown and targeted insertion of a CAR expression cassette at the same site.

The use of rAAV in this study was based on previous seminal work demonstrating its inherent capacity to facilitate HDR [reviewed in (*22*, *23*)]. Although the precise mechanisms that promote this process remain to be defined, rAAV gene targeting requires homologous recombination pathway proteins including RAD51/RAD54 (*24*) and properties specific to the structure or cellular processing of the single-stranded AAV genome (*25*). Additionally, as donor DNA is rate-limiting in driving HDR, the capacity to generate very high titer vector stocks combined with the limited toxicity of rAAV in most cell types provides the opportunity to drive mass action donor effects via delivery of very large numbers of viral genomes. Recently, several groups have leveraged these initial observations showing that after a nuclease-mediated DSB, rAAV-mediated HDR is markedly enhanced (>100-fold) in transformed cell lines, primary fibroblasts, or in vivo after liver-directed delivery (*26*–*32*). Although editing efficiencies of 1 to 10% were reported in most studies, levels as high as 65% were observed in the U2OS osteosarcoma line (*27*) after co-delivery of nuclease and donor in a single rAAV at an MOI similar to that used in our study. Application of these promising approaches in primary cells has been limited, in part, by identification of serotypes that efficiently transduce hematopoietic cell populations. We screened a panel of scAAV vectors containing a robust internal promoter driving GFP reporter gene expression and identified serotype 6 as optimal for targeting of both human primary T cells and $CD34^+$ progenitors. Although our serotype findings in $CD34^+$ cells differ from earlier studies (*33*, *34*), they are consistent with work from another group (*35*, *36*). On the basis of the serotype screen, we used AAV6 to successfully apply rAAV donor delivery in primary cells. In addition to templating targeted gene addition, rAAV also exhibits nonspecific integration at DNA break sites (*37*). Although this feature is prominent in transformed cell lines, reaching 20 to 30%, for example, in the osteosarcoma line described above (*27*), we found no evidence, on the basis of flow cytometry, for integration of AAV lacking homology arms in T cells in the absence of nuclease delivery. Low BFP reporter expression (~10-fold below HDR rates) was stably maintained, however, using control AAV with nuclease co-delivery, consistent with on-target AAV insertion. Notably, on the basis of genomic PCR analysis, targeted insertion was not observed after co-delivery of megaTAL and AAV donors with relevant homology arms, suggesting that HDR likely outcompetes random capture events. Our data cannot, however, exclude the possibility that non–HDR-directed integration of AAV occurs, either on-target at *CCR5* or off-target at the highly similar *CCR2* locus or other sites. Such integrations are unlikely to be any less safe than delivering CAR therapies by randomly integrating retroviruses, a method used in clinical trials without evidence of insertional mutagenesis [reviewed in (*38*)].

A key feature unique to the megaTAL platform is generation of DSB with 3′ DNA overhangs. We speculate that increased HDR rates at the *CCR5* target site using the CCR5-megaTAL reflect a platform-specific bias in repair pathway choice due to differences in DNA processing required to promote HDR and/or involvement of single-strand annealing pathways. However, to fully address this idea will require comparison of HDR efficiency at additional target sites using alternative TALENs, as well as other FOK1-based nucleases (ZFNs) and blunt-end cutters including Cas9/CRISPR reagents. Despite our limited mechanistic understanding, the efficiency of HDR mediated by the CCR5-megaTAL at this target site and the ability to deliver this nuclease from a single mRNA therapeutic validate consideration of this nuclease for clinical translation.

As an initial test for clinically relevant HDR gene-editing applications in HIV, we used several alternative gene expression cassettes including the C46 peptide and disease-relevant CAR constructs. We paired these knock-in cassettes with *CCR5* gene disruption. The *CCR5* disruption rates obtained with megaTAL or TALEN mRNA delivery were equivalent or superior to previous in vitro studies and as well as a ZFN-based clinical trial (*5*). We succeeded in pairing high-efficiency disruption with targeted integration of therapeutic gene cassettes, with unselected HDR efficiencies of ~8 to 30%. Variability in HDR efficiencies between viral constructs was partially explained by homology arm length (fig. S9) and was also affected by viral titer and size of nonhomologous insert; an important goal for clinical vectors will be to optimize these parameters of the donor template, as well as features of the therapeutic cassette that affect mRNA transport and stability. In our candidate anti–HIV-CAR, we included a cis-linked, clinically relevant surface peptide (*18*). This allowed us to enrich gene-modified T cells by using an anti-CD34 antibody and provides the capacity for subsequent specific in vivo depletion of modified T cells with an anti–CD20 mAb—an approach readily applicable to other therapeutic cassettes. We demonstrated in vitro functional activity using both CAR knock-in constructs. The MND, a retroviral promoter engineered to

resist transcriptional silencing (*39*, *40*), was used to achieve robust and stable transgene expression in lymphocytes. Although this promoter has been shown to be safe and effective in a clinical gene therapy trial (*41*), future therapeutics may use natural mammalian promoters or include insulators to reduce the potential for insertional mutagenesis or transcriptional silencing (*42*). It will also be important to determine whether *CCR5* site-specific integration manifests unanticipated safety concerns beyond CCR5 disruption alone. Although further work is required to assess sustained in vivo activity of these edited T cell populations, our capacity to achieve one-step, high-level modification and *CCR5* disruption is likely to be rapidly translatable into clinical application. For example, on the basis of the now well-documented activity of anti–CD19-CAR T cells [reviewed in (*43*)], the capacity to endow patient T cells with both resistance to HIV and the capacity to target B cell tumors represent a potential therapeutic for malignant complications encountered in HIV subjects.

We also applied our co-delivery methods to promote HDR in mobilized human $CD34^+$ PBSCs, a cell population relevant to clinical application across a wide range of hematopoietic disorders. We observed HDR rates of ~14% across multiple independent donors using co-delivery of megaTAL mRNA and rAAV. Although significantly less robust than in primary T cells, this rate is similar to previous work with ZFN mRNA and IDLV donor co-delivery to edit human cord blood– or bone marrow–derived $CD34^+$ cells (*11*, *12*). However, the rate at which we are successfully editing and maintaining the pluripotency of true HSCs within this population remains to be determined. Notably, our co-delivery approach in $CD34^+$ cells promoted substantially greater cell toxicity than in primary T cells, similar to results reported with ZFN and TALEN editing. Optimization of HDR in $CD34^+$ cells using this and other approaches [including Cas9 with dual-guide RNAs for efficient gene disruption (*20*)] will likely require a combinatorial manipulation of cell culture parameters to influence cell cycle and DNA repair pathway choice. Additionally, application of AAV serotypes with improved HSC transduction (*34*) and/or additional screening of recombinant serotypes may also facilitate editing outcomes.

In summary, we have established highly efficient methods to achieve targeted recombination within primary human hematopoietic cells by using co-delivery of megaTAL or TALEN-encoding mRNA and rAAV donor template. Although the packaging capacity of rAAV may limit some applications of this method, our findings highlight its potential for use in gene editing to engineer T cell products with a range of clinically relevant features and suggest that this platform may be translatable for use with alternative nucleases and cell types.

MATERIALS AND METHODS

Experimental design (objectives, design, and prespecified components)

The objective of this study was to develop a protocol for directing the integration of exogenous coding sequences into the *CCR5* locus of primary human T cells. Additional aims included assessing the impact of this gene editing on the homeostasis and cytotoxic T cell killing function in gene-edited cells and testing gene-editing reagents in adult human mobilized $CD34^+$ peripheral blood mononuclear cells (PBMCs). We first performed pilot experiments to optimize our gene-editing protocols in primary T cells and determined sample sizes needed to achieve an 80% statistical power at a P value of 0.05 to detect differences in HDR rates by flow cytometry detection of stable GFP expression. For NSG experiments, we calculated the sample size needed to detect a 1 SD change in the number of $CD4^+$ cells obtained at the end of the experiment with an 80% power and a P value of 0.05.

Nuclease design

The *CCR5*-targeting HE was identified and engineered on the basis of previously described methodologies (*13*, *44*). After yeast-based selection, the HE was assembled with a 10.5–repeat variable diresidue (RVD) TAL array as previously described (*7*) to generate the megaTAL enzyme (fig. S1). The resulting megaTAL enzyme recognized a 38-bp stretch in the sixth transmembrane domain of the *CCR5* gene (Fig. 1). The *CCR5*-specific TALEN pair was assembled with a Golden Gate cloning strategy (*45*) into a pthXO1 scaffold truncated at positions N154 and C63 as described (*46*). The *Xanthomonas* pthXo1 Golden Gate destination ORF and an RVD plasmid library were a gift from D. Voytas. The final TALEN pair and the megaTAL nucleases were cloned into a basic mRNA expression vector.

Production of recombinant AAV and lentiviral vectors

See Supplementary Materials for details of AAV and lentiviral constructs. AAV stocks were produced by triple transfection of AAV vector, serotype helper, and adenoviral helper [HGT1-adeno] plasmids in HEK 293T cells. Transfected cells were collected 48 hours later, lysed by freeze-thaw, benzonase-treated, and purified over iodixanol density gradient as previously described (*47*). Titers of the viral stocks were determined by qPCR of AAV genomes (*48*) and ranged from 1×10^{11} to 1×10^{12} per microliter. Lentivirus (LV) was prepared as described (*49*). Titers for IDLVs were determined with Lenti-X p24 Rapid Titer ELISA Kit (Clontech) according to the manufacturer's instructions.

Primary human T cell gene editing

T cells were thawed using drop-wise addition of cold deoxyribonuclease (DNAse) I buffer [phosphate-buffered saline (PBS), 5 mM $MgCl_2$, DNase I (20 Kunitz U/ml) (EMD-Millipore)], followed by centrifugation. Cells were resuspended at 1×10^6 live cells/ml in T cell growth medium (basic culture medium supplemented with IL-2, IL-7, and IL-15 at 50, 5, and 5 ng/ml, respectively) and stimulated by using CD3/CD28 beads (Dynabeads, Life Technologies) for 48 hours at a 1:1 cell-bead ratio. Beads were then removed, and cells were allowed to rest in T cell growth medium for 16 hours at 5×10^5 cells/ml. Next, cells were electroporated with mRNA using the Neon Transfection System and 10-μl tip as follows. Cells were washed twice with PBS, resuspended in Neon Buffer T at a density of 2.4×10^7 cells/ml, then 1 μg of mRNA (CCR5-megaTAL and BFP) or 2 μg of mRNA (1 μg of each CCR5-TALEN half-site) was added for every 2.5×10^5 to 3×10^5 cells. After mixing, cells were electroporated (1400 V, 10 ms, and three pulses) and immediately dispensed into 200 μl of prewarmed T cell growth medium in a 96-well plate. For samples transduced with AAV, AAV was added to the culture 2 to 4 hours after electroporation, followed by continued 30°C incubation for 20 additional hours. AAV donor was added as 20% of the final culture volume regardless of titer (~1×10^5 MOI) to optimize HDR events, unless specified otherwise. Samples not transduced with AAV were cultured continuously at 30°C for 24 hours. Subsequently, edited cells were cultured using standard conditions (37°C and expanded in T cell growth medium, replenished as needed to maintain a density of ~1×10^6 cells/ml every 2 to 3 days).

To scale up editing of primary human T cells for transplant into NSG mice, we used the above editing procedure with the following modifications:

10 μg of CCR5-megaTAL mRNA was used to transfect 3×10^6 primary human $CD4^+$ T cells using the Neon Transfection Kit 100-μl tips (using the same electrical parameters as above). Cells were transduced 2 to 4 hours after electroporation by addition of 20% culture volume of AAV (6×10^5 MOI), returned to 30°C for 22 hours, then expanded in a G-Rex10 flask (Wilson Wolf Manufacturing). During expansion, 75% of the medium volume was exchanged every 3 to 4 days with fresh T cell growth medium. Eight days after electroporation, cells were collected, washed, and used for transplantation.

TCR spectratyping

Spectratypes of TCR Vβ CDR3 subfamilies present in gene-edited $CD4^+$ T cell samples were determined by the Immune Monitoring Core at the Fred Hutchinson Cancer Research Center using multiplex reverse transcription PCR as described (*50*). Complexity scores of each subfamily were determined as described (*51*).

Murine transplantation and analyses

NSG mice (Jackson Laboratory) were maintained in a specific pathogen–free Association for Assessment and Accreditation of Laboratory Animal Care–accredited facility in accordance with National Institutes of Health (NIH) *Guide for the Care and Use of Laboratory Animals* and the Seattle Children's Research Institute's Institutional Animal Care and Use Committee. Animals (8 to 15 weeks old) were injected intraperitoneally with 2×10^7 engineered T cells in PBS, monitored daily and weighed twice-weekly, and euthanized at 4 weeks after transplant for analysis of engrafted cells.

Adult human mobilized $CD34^+$ cell culture and transfection

Cryopreserved $CD34^+$ cells enriched from PBSC mobilized adult donors were obtained from the Core Center for Excellence in Hematology at the Fred Hutchinson Cancer Research Center. Cells were thawed as described above. After centrifugation, $CD34^+$ cells were resuspended to a concentration of 1×10^6 cells/ml in serum-free stem cell medium [StemSpan Medium (STEMCELL Technologies) with thrombopoietin, stem cell factor, IL-6, and FLT3 ligand (PeproTech), all at 100 ng/ml]. $CD34^+$ cells were prestimulated in this cytokine mix for 24 hour at 37°C, followed by the addition of the AAV (10% of culture volume) for 24 hour, washed with PBS, resuspended in Neon Buffer T at a density of 3×10^5 cells/ml, and transfected using 1 μg of mRNA for every 3×10^5 cells using the following settings: 1900 V, 20 ms, and 1 pulse. Cells were then dispensed into 3 ml of prewarmed stem cell medium in a six-well plate, and then incubated at 37°C. StemRegenin (1 ng/ml) (Cellagen Technology) (*52*) was added 24 hours after gene editing and on alternate days in culture. Analysis of GFP and BFP expression was performed 4 and 10 days after gene editing. gDNA was extracted from cells at each condition on day 10 for molecular analyses of HDR.

T cell killing assays

An expression cassette for CD19-CAR.2A.BFP was targeted to the *CCR5* locus of $CD3^+$ T cells using the above gene-editing protocol, grown in T cell growth medium for 9 days, and FACS-sorted into BFP-positive and BFP-negative fractions. Sorted cells were expanded for 1 week in T cell growth medium in a T25 flask with OKT3 antibody (30 ng/ml), 25 million irradiated human PBMCs, and 5 million irradiated transformed lymphoblastoid cell lines (*53*) as described (*54*). Target and control (CD19 or BCMA expressing, respectively) cells were generated by LV transduction of K562 cells using either pRRL.MND.CD19.2A.GFP or pRRL.MND.mBCMA.2A.iRFP, respectively. For killing assays, BFP-positive or BFP-negative T cells (effector) were plated in T cell growth medium in a 96-well plate with a 1:1 mix of CD19/GFP^+K562 (target) and 5×10^4 mBCMA/$iRFP^+$ K562 cells at effector to target ratios of 1:1, 3:1, 5:1, and 10:1. After 48 hours, cells were analyzed by FACS. CAR-mediated killing was reported as a decrease in the percentage of GFP^+ target cells relative to $iRFP^+$ control cells.

$CD3^+$ T cells that underwent *CCR5* gene editing using the AAV.CCR5.HIV-CAR.2A.RQR8 donor template were enriched by flow sorting $RQR8^+$ cells (labeled with anti-human CD34 followed by goat anti-mouse IgG1-PE secondary; table S1) and grown as described above. $CD3^+$ T cells with the CD19-CAR.2A.BFP construct were generated in parallel and enriched by sorting on BFP. To assess activation of HIV-CAR–expressing cells, edited cells were cocultured at a 1:1 ratio with either a chronically HIV-infected T cell line (ACH-2) or the parental control, A3.01 T cell line (final concentration, 1×10^6 cells/ml). Before use in this assay, ACH-2 and A3.01 cells were grown separately for 24 hours in T cell culture medium with 1 μM phorbol 12-myristate 13-acetate and antiretroviral therapy (tenofovir, azidothymidine, and nevirapine, 20 μM each; NIH AIDS Reagent Program). After 24 hours in coculture-edited T cells were stained using anti-CD137, followed by LIVE/DEAD Fixable Near-IR Viability Stain, incubated for 15 min in 4% paraformaldehyde and analyzed by flow cytometry.

Statistical analysis

Statistical analyses were performed with Prism 6 (GraphPad Software). Data are shown as means ± SEM unless otherwise noted. Tests of statistical significance were performed using the unpaired two-tailed Student's *t* test; where noted, we corrected for multiple comparisons using the Holm-Sidak method with $\alpha = 5.0\%$. For multiple comparisons of normally distributed data, statistical analysis was determined with a two-way analysis of variance using Tukey's multiple comparison test, $\alpha = 5.0\%$.

SUPPLEMENTARY MATERIALS

www.sciencetranslationalmedicine.org/cgi/content/full/7/307/307ra156/DC1
Materials and Methods
Fig. S1. CCR5-megaTAL amino acid sequence.
Fig. S2. Spectrum of indels at *CCR5* target site in human T cells after megaTAL or TALEN treatment.
Fig. S3. Robust transduction of human primary hematopoietic cells using AAV6.
Fig. S4. Sequence analyses verifying seamless HDR using AAV.CCR5.GFP donor template.
Fig. S5. Comparison of transfection, transduction, and HDR events using *CCR5* gene–editing reagents in CD3, CD4, and CD8 T cells.
Fig. S6. Efficacy of IDLV delivered donor template for HDR gene editing.
Fig. S7. Evaluation of off-target editing by *CCR5* nucleases in primary human T cells.
Fig. S8. TCR spectratyping demonstrates maintenance of TCR complexity in gene-edited T cells.
Fig. S9. Variation of HDR rates with *CCR5* homology arm size.
Table S1. Antibody sources.
References (*55*–*62*)

REFERENCES AND NOTES

1. H. M. Naif, Pathogenesis of HIV Infection. *Infect. Dis. Rep.* **5**, e6 (2013).
2. M. Dean, M. Carrington, C. Winkler, G. A. Huttley, M. W. Smith, R. Allikmets, J. J. Goedert, S. P. Buchbinder, E. Vittinghoff, E. Gomperts, S. Donfield, D. Vlahov, R. Kaslow, A. Saah, C. Rinaldo, R. Detels, S. J. O'Brien, Genetic restriction of HIV-1 infection and progression to AIDS by a deletion allele of the *CKR5* structural gene. *Science* **273**, 1856–1862 (1996).
3. R. Liu, W. A. Paxton, S. Choe, D. Ceradini, S. R. Martin, R. Horuk, M. E. MacDonald, H. Stuhlmann, R. A. Koup, N. R. Landau, Homozygous defect in HIV-1 coreceptor accounts for resistance of some multiply-exposed individuals to HIV-1 infection. *Cell* **86**, 367–377 (1996).
4. M. Samson, F. Libert, B. J. Doranz, J. Rucker, C. Liesnard, C.-M. Farber, S. Saragosti, C. Lapoumèroulie, J. Cognaux, C. Forceille, G. Muyldermans, C. Verhofstede, G. Burtonboy, M. Georges, T. Imai,

S. Rana, Y. Yi, R. J. Smyth, R. G. Collman, R. W. Doms, G. Vassart, M. Parmentier, Resistance to HIV-1 infection in Caucasian individuals bearing mutant alleles of the CCR-5 chemokine receptor gene. *Nature* **382**, 722–725 (1996).
5. P. Tebas, D. Stein, W. W. Tang, I. Frank, S. Q. Wang, G. Lee, S. K. Spratt, R. T. Surosky, M. A. Giedlin, G. Nichol, M. C. Holmes, P. D. Gregory, D. G. Ando, M. Kalos, R. G. Collman, G. Binder-Scholl, G. Plesa, W. T. Hwang, B. L. Levine, C. H. June, Gene editing of *CCR5* in autologous CD4 T cells of persons infected with HIV. *N. Engl. J. Med.* **370**, 901–910 (2014).
6. R. A. Voit, M. A. McMahon, S. L. Sawyer, M. H. Porteus, Generation of an HIV resistant T-cell line by targeted "stacking" of restriction factors. *Mol. Ther.* **21**, 786–795 (2013).
7. S. Boissel, J. Jarjour, A. Astrakhan, A. Adey, A. Gouble, P. Duchateau, J. Shendure, B. L. Stoddard, M. T. Certo, D. Baker, A. M. Scharenberg, megaTALs: A rare-cleaving nuclease architecture for therapeutic genome engineering. *Nucleic Acids Res.* **42**, 2591–2601 (2014).
8. T. Tsuji, Y. Niida, Development of a simple and highly sensitive mutation screening system by enzyme mismatch cleavage with optimized conditions for standard laboratories. *Electrophoresis* **29**, 1473–1483 (2008).
9. E. K. Brinkman, T. Chen, M. Amendola, B. van Steensel, Easy quantitative assessment of genome editing by sequence trace decomposition. *Nucleic Acids Res.* **42**, e168 (2014).
10. M. T. Certo, B. Y. Ryu, J. E. Annis, M. Garibov, J. Jarjour, D. J. Rawlings, A. M. Scharenberg, Tracking genome engineering outcome at individual DNA breakpoints. *Nat. Methods* **8**, 671–676 (2011).
11. M. D. Hoban, G. J. Cost, M. C. Mendel, Z. Romero, M. L. Kaufman, A. V. Joglekar, M. Ho, D. Lumaquin, D. Gray, G. R. Lill, A. R. Cooper, F. Urbinati, S. Senadheera, A. Zhu, P.-Q. Liu, D. E. Paschon, L. Zhang, E. J. Rebar, A. Wilber, X. Wang, P. D. Gregory, M. C. Holmes, A. Reik, R. P. Hollis, D. B. Kohn, Correction of the sickle cell disease mutation in human hematopoietic stem/progenitor cells. *Blood* **125**, 2597–2604 (2015).
12. P. Genovese, G. Schiroli, G. Escobar, T. Di Tomaso, C. Firrito, A. Calabria, D. Moi, R. Mazzieri, C. Bonini, M. C. Holmes, P. D. Gregory, M. van der Burg, B. Gentner, E. Montini, A. Lombardo, L. Naldini, Targeted genome editing in human repopulating haematopoietic stem cells. *Nature* **510**, 235–240 (2014).
13. Y. Wang, I. F. Khan, S. Boissel, J. Jarjour, J. Pangallo, S. Thyme, D. Baker, A. M. Scharenberg, D. J. Rawlings, Progressive engineering of a homing endonuclease genome editing reagent for the murine X-linked immunodeficiency locus. *Nucleic Acids Res.* **42**, 6463–6475 (2014).
14. E. E. Perez, J. Wang, J. C. Miller, Y. Jouvenot, K. A. Kim, O. Liu, N. Wang, G. Lee, V. V. Bartsevich, Y.-L. Lee, D. Y. Guschin, I. Rupniewski, A. J. Waite, C. Carpenito, R. G. Carroll, J. S. Orange, F. D. Urnov, E. J. Rebar, D. Ando, P. D. Gregory, J. L. Riley, M. C. Holmes, C. H. June, Establishment of HIV-1 resistance in $CD4^+$ T cells by genome editing using zinc-finger nucleases. *Nat. Biotechnol.* **26**, 808–816 (2008).
15. M. Egelhofer, G. Brandenburg, H. Martinius, P. Schult-Dietrich, G. Melikyan, R. Kunert, C. Baum, I. Choi, A. Alexandrov, D. von Laer, Inhibition of human immunodeficiency virus type 1 entry in cells expressing gp41-derived peptides. *J. Virol.* **78**, 568–575 (2004).
16. M. Hildinger, M. T. Dittmar, P. Schult-Dietrich, B. Fehse, B. S. Schnierle, S. Thaler, G. Stiegler, R. Welker, D. von Laer, Membrane-anchored peptide inhibits human immunodeficiency virus entry. *J. Virol.* **75**, 3038–3042 (2001).
17. L. M. Walker, M. Huber, K. J. Doores, E. Falkowska, R. Pejchal, J.-P. Julien, S.-K. Wang, A. Ramos, P.-Y. Chan-Hui, M. Moyle, J. L. Mitcham, P. W. Hammond, O. A. Olsen, P. Phung, S. Fling, C.-H. Wong, S. Phogat, T. Wrin, M. D. Simek, W. C. Koff, I. A. Wilson, D. R. Burton, P. Poignard; Protocol G Principal Investigators, Broad neutralization coverage of HIV by multiple highly potent antibodies. *Nature* **477**, 466–470 (2011).
18. B. Philip, E. Kokalaki, L. Mekkaoui, S. Thomas, K. Straathof, B. Flutter, V. Marin, T. Marafioti, R. Chakraverty, D. Linch, S. A. Quezada, K. S. Peggs, M. Pule, A highly compact epitope-based marker/suicide gene for easier and safer T-cell therapy. *Blood* **124**, 1277–1287 (2014).
19. F. D. Urnov, J. C. Miller, Y.-L. Lee, C. M. Beausejour, J. M. Rock, S. Augustus, A. C. Jamieson, M. H. Porteus, P. D. Gregory, M. C. Holmes, Highly efficient endogenous human gene correction using designed zinc-finger nucleases. *Nature* **435**, 646–651 (2005).
20. P. K. Mandal, L. M. R. Ferreira, R. Collins, T. B. Meissner, C. L. Boutwell, M. Friesen, V. Vrbanac, B. S. Garrison, A. Stortchevoi, D. Bryder, K. Musunuru, H. Brand, A. M. Tager, T. M. Allen, M. E. Talkowski, D. J. Rossi, C. A. Cowan, Efficient ablation of genes in human hematopoietic stem and effector cells using CRISPR/Cas9. *Cell Stem Cell* **15**, 643–652 (2014).
21. B. Berdien, U. Mock, D. Atanackovic, B. Fehse, TALEN-mediated editing of endogenous T-cell receptors facilitates efficient reprogramming of T lymphocytes by lentiviral gene transfer. *Gene Ther.* **21**, 539–548 (2014).
22. P. C. Hendrie, D. W. Russell, Gene targeting with viral vectors. *Mol. Ther.* **12**, 9–17 (2005).
23. A. Vasileva, R. Jessberger, Precise hit: Adeno-associated virus in gene targeting. *Nat. Rev. Microbiol.* **3**, 837–847 (2005).
24. A. Vasileva, R. M. Linden, R. Jessberger, Homologous recombination is required for AAV-mediated gene targeting. *Nucleic Acids Res.* **34**, 3345–3360 (2006).
25. R. K. Hirata, D. W. Russell, Design and packaging of adeno-associated virus gene targeting vectors. *J. Virol.* **74**, 4612–4620 (2000).
26. B. L. Ellis, M. L. Hirsch, S. N. Porter, R. J. Samulski, M. H. Porteus, Zinc-finger nuclease-mediated gene correction using single AAV vector transduction and enhancement by food and drug Administration-approved drugs. *Gene Ther.* **20**, 35–42 (2013).
27. K. Gellhaus, T. I. Cornu, R. Heilbronn, T. Cathomen, Fate of recombinant adeno-associated viral vector genomes during DNA double-strand break-induced gene targeting in human cells. *Hum. Gene Ther.* **21**, 543–553 (2010).
28. E. M. Händel, K. Gellhaus, K. Khan, C. Bednarski, T. I. Cornu, F. Müller-Lerch, R. M. Kotin, R. Heilbronn, T. Cathomen, Versatile and efficient genome editing in human cells by combining zinc-finger nucleases with adeno-associated viral vectors. *Hum. Gene Ther.* **23**, 321–329 (2012).
29. M. L. Hirsch, L. Green, M. H. Porteus, R. J. Samulski, Self-complementary AAV mediates gene targeting and enhances endonuclease delivery for double-strand break repair. *Gene Ther.* **17**, 1175–1180 (2010).
30. H. Li, V. Haurigot, Y. Doyon, T. Li, S. Y. Wong, A. S. Bhagwat, N. Malani, X. M. Anguela, R. Sharma, L. Ivanciu, S. L. Murphy, J. D. Finn, F. R. Khazi, S. Zhou, D. E. Paschon, E. J. Rebar, F. D. Bushman, P. D. Gregory, M. C. Holmes, K. A. High, In vivo genome editing restores haemostasis in a mouse model of haemophilia. *Nature* **475**, 217–221 (2011).
31. D. G. Miller, L. M. Petek, D. W. Russell, Human gene targeting by adeno-associated virus vectors is enhanced by DNA double-strand breaks. *Mol. Cell Biol.* **23**, 3550–3557 (2003).
32. M. H. Porteus, T. Cathomen, M. D. Weitzman, D. Baltimore, Efficient gene targeting mediated by adeno-associated virus and DNA double-strand breaks. *Mol. Cell Biol.* **23**, 3558–3565 (2003).
33. B. L. Ellis, M. L. Hirsch, J. C. Barker, J. P. Connelly, R. J. Steininger III, M. H. Porteus, A survey of ex vivo/in vitro transduction efficiency of mammalian primary cells and cell lines with nine natural adeno-associated virus (AAV1-9) and one engineered adeno-associated virus serotype. *Virol. J.* **10**, 74 (2013).
34. L. J. Smith, T. Ul-Hasan, S. K. Carvaines, K. Van Vliet, E. Yang, K. K. Wong Jr., M. Agbandje-McKenna, S. Chatterjee, Gene transfer properties and structural modeling of human stem cell-derived AAV. *Mol.Ther.* **22**, 1625–1634 (2014).
35. L. Song, M. A. Kauss, E. Kopin, M. Chandra, T. Ul-Hasan, E. Miller, G. R. Jayandharan, A. E. Rivers, G. V. Aslanidi, C. Ling, B. Li, W. Ma, X. Li, L. M. Andino, L. Zhong, A. F. Tarantal, M. C. Yoder, K. K. Wong Jr., M. Tan, S. Chatterjee, A. Srivastava, Optimizing the transduction efficiency of capsid-modified AAV6 serotype vectors in primary human hematopoietic stem cells in vitro and in a xenograft mouse model in vivo. *Cytotherapy* **15**, 986–998 (2013).
36. L. Song, X. Li, G. R. Jayandharan, Y. Wang, G. V. Aslanidi, C. Ling, L. Zhong, G. Gao, M. C. Yoder, C. Ling, M. Tan, A. Srivastava, High-efficiency transduction of primary human hematopoietic stem cells and erythroid lineage-restricted expression by optimized AAV6 serotype vectors in vitro and in a murine xenograft model in vivo. *PLOS One* **8**, e58757 (2013).
37. D. G. Miller, L. M. Petek, D. W. Russell, Adeno-associated virus vectors integrate at chromosome breakage sites. *Nat. Genet.* **36**, 767–773 (2004).
38. C. H. June, S. R. Riddell, T. N. Schumacher, Adoptive cellular therapy: A race to the finish line. *Sci. Transl. Med.* **7**, 280ps287 (2015).
39. P.-M. Challita, D. Skelton, A. El-Khoueiry, X.-J. Yu, K. Weinberg, D. B. Kohn, Multiple modifications in *cis* elements of the long terminal repeat of retroviral vectors lead to increased expression and decreased DNA methylation in embryonic carcinoma cells. *J. Virol.* **69**, 748–755 (1995).
40. S. Halene, L. Wang, R. M. Cooper, D. C. Bockstoce, P. B. Robbins, D. B. Kohn, Improved expression in hematopoietic and lymphoid cells in mice after transplantation of bone marrow transduced with a modified retroviral vector. *Blood* **94**, 3349–3357 (1999).
41. N. Cartier, S. Hacein-Bey-Abina, C. C. Bartholomae, G. Veres, M. Schmidt, I. Kutschera, M. Vidaud, U. Abel, L. Dal-Cortivo, L. Caccavelli, N. Mahlaoui, V. Kiermer, D. Mittelstaedt, C. Bellesme, N. Lahlou, F. Lefrère, S. Blanche, M. Audit, E. Payen, P. Leboulch, B. l'Homme1, P. Bougnères, C. Von Kalle, A. Fischer, M. Cavazzana-Calvo, P. Aubourg, Hematopoietic stem cell gene therapy with a lentiviral vector in X-linked adrenoleukodystrophy. *Science* **326**, 818–823 (2009).
42. R. M. Koldej, G. Carney, M. M. Wielgosz, S. Zhou, J. Zhan, B. P. Sorrentino, A. W. Nienhuis, Comparison of insulators and promoters for expression of the Wiskott–Aldrich syndrome protein using lentiviral vectors. *Hum. Gene Ther. Clin. Dev.* **24**, 77–85 (2013).
43. S. Gill, C. H. June, Going viral: Chimeric antigen receptor T-cell therapy for hematological malignancies. *Immunol. Rev.* **263**, 68–89 (2015).
44. J. Jarjour, H. West-Foyle, M. T. Certo, C. G. Hubert, L. Doyle, M. M. Getz, B. L. Stoddard, A. M. Scharenberg, High-resolution profiling of homing endonuclease binding and catalytic specificity using yeast surface display. *Nucleic Acids Res.* **37**, 6871–6880 (2009).
45. T. Cermak, E. L. Doyle, M. Christian, L. Wang, Y. Zhang, C. Schmidt, J. A. Baller, N. V. Somia, A. J. Bogdanove, D. F. Voytas, Efficient design and assembly of custom TALEN and other TAL effector-based constructs for DNA targeting. *Nucleic Acids Res.* **39**, e82 (2011).
46. J. C. Miller, S. Tan, G. Qiao, K. A. Barlow, J. Wang, D. F. Xia, X. Meng, D. E. Paschon, E. Leung, S. J. Hinkley, G. P. Dulay, K. L. Hua, I. Ankoudinova, G. J. Cost, F. D. Urnov, H. S. Zhang, M. C. Holmes, L. Zhang, P. D. Gregory, E. J. Rebar, A TALE nuclease architecture for efficient genome editing. *Nat. Biotechnol.* **29**, 143–148 (2011).
47. I. F. Khan, R. K. Hirata, D. W. Russell, AAV-mediated gene targeting methods for human cells. *Nat. Protoc.* **6**, 482–501 (2011).
48. C. Aurnhammer, M. Haase, N. Muether, M. Hausl, C. Rauschhuber, I. Huber, H. Nitschko, U. Busch, A. Sing, A. Ehrhardt, A. Baiker, Universal real-time PCR for the detection and quantification of adeno-associated virus serotype 2-derived inverted terminal repeat sequences. *Hum.Gene Ther. Methods* **23**, 18–28 (2012).

49. X. Wang, S. C. Shin, A. F. Chiang, I. Khan, D. Pan, D. J. Rawlings, C. H. Miao, Intraosseous delivery of lentiviral vectors targeting factor VIII expression in platelets corrects murine hemophilia A. *Mol. Ther.* **23**, 617–626 (2015).
50. Y. Akatsuka, E. G. Martin, A. Madonik, A. A. Barsoukov, J. A. Hansen, Rapid screening of T-cell receptor (TCR) variable gene usage by multiplex PCR: Application for assessment of clonal composition. *Tissue Antigens* **53**, 122–134 (1999).
51. A. Konno, K. Okada, K. Mizuno, M. Nishida, S. Nagaoki, T. Toma, T. Uehara, K. Ohta, Y. Kasahara, H. Seki, A. Yachie, S. Koizumi, CD8αα memory effector T cells descend directly from clonally expanded $CD8\alpha^{+}\beta^{high}$ TCRαβ T cells in vivo. *Blood* **100**, 4090–4097 (2002).
52. A. E. Boitano, J. Wang, R. Romeo, L. C. Bouchez, A. E. Parker, S. E. Sutton, J. R. Walker, C. A. Flaveny, G. H. Perdew, M. S. Denison, P. G. Schultz, M. P. Cooke, Aryl hydrocarbon receptor antagonists promote the expansion of human hematopoietic stem cells. *Science* **329**, 1345–1348 (2010).
53. S. Terakura, T. N. Yamamoto, R. A. Gardner, C. J. Turtle, M. C. Jensen, S. R. Riddell, Generation of CD19-chimeric antigen receptor modified $CD8^{+}$ T cells derived from virus-specific central memory T cells. *Blood* **119**, 72–82 (2012).
54. J. Wang, O. W. Press, C. G. Lindgren, P. Greenberg, S. Riddell, X. Qian, C. Laugen, A. Raubitschek, S. J. Forman, M. C. Jensen, Cellular immunotherapy for follicular lymphoma using genetically modified CD20-specific $CD8^{+}$ cytotoxic T lymphocytes. *Mol. Ther.* **9**, 577–586 (2004).
55. E. A. Rutledge, C. L. Halbert, D. W. Russell, Infectious clones and vectors derived from adeno-associated virus (AAV) serotypes other than AAV type 2. *J. Virol.* **72**, 309–319 (1998).
56. D. Grimm, J. S. Lee, L. Wang, T. Desai, B. Akache, T. A. Storm, M. A. Kay, In vitro and in vivo gene therapy vector evolution via multispecies interbreeding and retargeting of adeno-associated viruses. *J. Virol.* **82**, 5887–5911 (2008).
57. D. E. Bowles, S. W. J. McPhee, C. Li, S. J. Gray, J. J. Samulski, A. S. Camp, J. Li, B. Wang, P. E. Monahan, J. E. Rabinowitz, J. C. Grieger, L. Govindasamy, M. Agbandje-McKenna, X. Xiao, R. J. Samulski, Phase 1 gene therapy for Duchenne muscular dystrophy using a translational optimized AAV vector. *Mol. Ther.* **20**, 443–455 (2012).
58. N. Levitt, D. Briggs, A. Gil, N. J. Proudfoot, Definition of an efficient synthetic poly(A) site. *Genes Dev.* **3**, 1019–1025 (1989).
59. M. C. Milone, J. D. Fish, C. Carpenito, R. G. Carroll, G. K. Binder, D. Teachey, M. Samanta, M. Lakhal, B. Gloss, G. Danet-Desnoyers, D. Campana, J. L. Riley, S. A. Grupp, C. H. June, Chimeric receptors containing CD137 signal transduction domains mediate enhanced survival of T cells and increased antileukemic efficacy in vivo. *Mol. Ther.* **17**, 1453–1464 (2009).
60. A. Buchacher, R. Predl, K. Strutzenberger, W. Steinfellner, A. Trkola, M. Purtscher, G. Gruber, C. Tauer, F. Steindl, A. Jungbauer, H. Katinger, Generation of human monoclonal antibodies against HIV-1 proteins; electrofusion and Epstein-Barr virus transformation for peripheral blood lymphocyte immortalization. *AIDS Res. Hum. Retroviruses* **10**, 359–369 (1994).
61. M. Purtscher, A. Trkola, A. Grassauer, P. M. Schulz, A. Klima, S. Döpper, G. Gruber, A. Buchacher, T. Muster, H. Katinger, Restricted antigenic variability of the epitope recognized by the neutralizing gp41 antibody 2F5. *AIDS* **10**, 587–593 (1996).
62. M. Purtscher, A. Trkola, G. Gruber, A. Buchacher, R. Predl, F. Steindl, C. Tauer, R. Berger, N. Barrett, A. Jungbauer, H. Katinger, A broadly neutralizing human monoclonal antibody against gp41 of human immunodeficiency virus type 1. *AIDS Res. Hum. Retroviruses* **10**, 1651–1658 (1994).

Acknowledgments: We thank M. Withrow for assistance with the manuscript and the members of the Rawlings and Scharenberg laboratories and the Seattle Children's Program for Cell and Gene Therapy for helpful discussions. We thank the following for the gifts of reagents used in this work: D. Russell (AAV6 helper plasmid), J.-S. Lee (HGT1-adeno and AAV1, AAV2, AAV5, and AAV8 helper plasmids), J. T. Gray (pscAAV.GFP and pAAV.GFP), and D. Voytas (pthXo1 Golden Gate destination ORF and RVD plasmid library). **Funding:** This work was supported by the National Heart, Lung, and Blood Institute and National Institute of General Medical Sciences of the NIH under award numbers RL1 HL092553, PL1 HL092557 (to D.J.R.), and R42 GM085876 (to A.A.). The content is solely the responsibility of the authors and does not necessarily represent the official views of the NIH. Additional support was provided by the Seattle Children's Program for Cell and Gene Therapy. **Author contributions:** B.D.S., G.S.R.I., K.S., G.C., M.H., I.F.K., S.S., Y.S., K.G., J.S., J.J., A.A., and T.A.W. generated novel molecular reagents and/or performed the experiments; B.D.S., G.S.R.I., K.S., G.C., M.H., I.F.K., S.S., T.A.W., A.M.S., and D.J.R. designed experiments; and K.S. and D.J.R. wrote the manuscript. **Competing interests:** A.A. is an employee and shareholder and A.M.S. a consultant and shareholder in Bluebird Bio. B.D.S. is currently an employee of Juno Therapeutics. All other authors declare that they have no competing interests. **Data and materials availability:** Materials described here will be provided upon request upon execution of a material transfer agreement with Seattle Children's Research Institute and/or Bluebird Bio.

Submitted 11 May 2015
Accepted 2 September 2015
Published 30 September 2015
10.1126/scitranslmed.aac5530

Citation: B. D. Sather, G. S. Romano Ibarra, K. Sommer, G. Curinga, M. Hale, I. F. Khan, S. Singh, Y. Song, K. Gwiazda, J. Sahni, J. Jarjour, A. Astrakhan, T. A. Wagner, A. M. Scharenberg, D. J. Rawlings, Efficient modification of *CCR5* in primary human hematopoietic cells using a megaTAL nuclease and AAV donor template. *Sci. Transl. Med.* **7**, 307ra156 (2015).